

# RECONFIGURABLE PARTICLE SEPARATION BY DYNAMIC ACOUSTIC FIELDS IN MICROFLUIDIC DEVICES

Gergely Simon, Jose Marques-Hueso, Marc P. Y. Desmulliez, Anne L. Bernassau

*Heriot-Watt University, School of Engineering and Physical Sciences, Edinburgh, U.K.  
a.bernassau@hw.ac.uk*

D. Roolvink, G. Burns, P. A. G. Cormack

*Strathclyde University, Department of Pure & Applied Chemistry, Glasgow, U.K.*

Marco A. B. Andrade

*University of São Paulo, Institute of Physics, São Paulo, Brazil*

Julien Reboud, Jonathan M. Cooper

*University of Glasgow, School of Engineering, Glasgow, U.K.*

Mathis O. Riehle

*University of Glasgow, Institute of Molecular Cell and Systems Biology, Glasgow, U.K.*

Advances in diagnostics, cell and stem cell technologies drive the development of application-specific tools for cell and particle separation. Acoustic micro-particle separation offers a promising avenue for label-free, high recovery, cell and particle separation and isolation in tissue engineering and targeted drug delivery. In this paper, we present two methods of separating particles in a microfluidic channel. The first method uses custom-made micro-particles and by changing the acoustic contrast factor, the micro-particles shift from acoustic node to antinodes, compared to commercialised micro-particles. The second method relies on shifting the acoustic standing wave in a pattern called dynamic acoustic field. We demonstrate that both methods separate particles up to 100%.

Keywords: acoustic radiation force, cell sorting.

---

## 1. Introduction

Contactless manipulation and sorting of particles and cells have diverse applications including sample preparation [1], target cell enrichment [2] and patterning for tissue engineering [3, 4]. Most of the active handling methods rely on a specific property of the targeted particles such as electric permittivity [5, 6] or magnetic permeability [7] and therefore cannot be applied to targets lacking these characteristics. Optical approaches [8, 9] overcome this limitation by enabling the manipulation of any kind of particles that differ in refractive index, but the bulky experimental setup comprising laser, optics and translational stage makes the operation cumbersome. Acoustic approaches are contactless and biocompatible [10] requiring no labelling of particles and therefore can be used for enrichment, separation or tweezing [11-13] without any adverse effects on cells or materials. Classical acoustic methods achieve particle or cell separation by generating a standing wave field inside the active area of the device [14-16]. Although these devices can be reconfigured for a specific target cell or particle by adjusting the applied voltage, the generated heat in the device will vary over the broad range of operating conditions, possibly limiting biological applications [17].

In recent years, dynamic acoustic approaches, where the radiation force changes with time, have gained increasing interest for particle manipulation. These methods allow reconfiguration of the acoustic field within the same device [18]. In its simplest form, the transducers can be switched on/off providing actuation for fluorescence-activated cell sorting (FACS) techniques [13, 19] or for patterning [20]. Switching the frequency between normal modes of resonance within a device allows manipulation [21] and sorting of particles [22]. This frequency mode switching technique has been further extended from binary separation to multichannel sorting in a surface acoustic wave device [23].

In this paper, we present two methods for separating micro-particles. The first method relies on tailored micro-particles and shifting the acoustic contrast factor. The second method uses dynamic acoustic standing wave fields and takes advantages of the different scaling forces applied on the micro-particles.

## 2. Method

### 2.1 Acoustic radiation force

When two opposing ultrasonic transducers are activated by the same sinusoidal signal, an acoustic standing wave pattern is formed. The spherical particles suspended in the fluid media between transducers scatter the acoustic field and give rise to the primary acoustic radiation force [24]:

$$F_r = -\left(\frac{\pi p_0^2 V_c \beta_w}{2\lambda}\right) \cdot \phi(\beta, \rho) \cdot \sin(2kx) \quad (1)$$

$$\phi(\beta, \rho) = \frac{5\rho_c - 2\rho_w}{2\rho_c + \rho_w} - \frac{\beta_c}{\beta_w} \quad (2)$$

$$F_v = -6\pi\eta Rv \quad (3)$$

where  $p_0$  is the acoustic pressure amplitude,  $V_c$  is the volume of the particle,  $\lambda$  is the wavelength,  $k$  is the wave number that is equal to  $2\pi/\lambda$ ,  $x$  is the distance from a pressure node,  $\rho_c$  and  $\rho_w$  are the densities of the particle and the fluid, respectively,  $\beta_c$  and  $\beta_w$  are the compressibility of the particle and the fluid, respectively,  $\eta$  is the medium viscosity,  $R$  is the particle radius, and  $v$  is the relative velocity.

The acoustic contrast factor, (2), represented by  $\phi$  in (1), depends on both the particle density ( $\rho_c$ ) and its compressibility ( $\beta_c$ ) in relation to the corresponding properties of the surrounding medium ( $\rho_w, \beta_w$ ).

Therefore the acoustic radiation force scales with the cube of the radius of the particle, and has a weak dependence on the density. Based on the particle parameters they can either have negative or positive acoustic contrast factor. Particles with positive contrast factor are pushed towards the pressure nodes by the acoustic radiation force, while particles with negative contrast factor agglomerate along the antinodes. This can be readily utilized for binary fractionation [25].

### 2.2. Dynamic acoustic standing waves

By electrically exciting the transducers, counter-propagating acoustic waves are generated. The propagating and counter-propagating waves interfere with one another and produce an acoustic standing wave field in the liquid medium enclosed between the 2 transducers. This standing wave field generates acoustic radiation forces on small particles, causing their migration to the pressure nodes for particles of positive acoustic contrast factor.

By introducing a phase shift between two transducers signals, the position of the pressure nodes

can be controlled and particles can be manipulated inside the fluid. In the dynamic acoustic standing wave method, the phase of one of the transducers is modulated, with a phase shift pattern shown in Fig. 1 (top graph). The first segment of this pattern is called the ramping time,  $t_{ramp}$ , where the phase of the signal supplied to one side of the device is changed gradually from  $0^\circ$  to  $360^\circ$  relative to that of the other side. The phase shift remains unchanged in the second segment, called the resting time  $t_{rest}$ ; this allows the particles to reach an equilibrium position. During the ramping time, the standing wave pattern moves laterally and the radiation force shifts the particles with the pressure nodes.

Since the acoustic radiation force (1) and viscous force (3) scale differently with the size of the particle, thus different sized particles will follow different trajectories (Fig. 1, bottom graph). If the ramping time is too short, none of the particles will be able to follow the apparent movement of the nodes preventing any separation. Similarly, when  $t_{ramp}$  is too long, all particles will follow the apparent movement of the nodes and again separation is prevented. By choosing  $t_{ramp}$  appropriately, separation of particles that differ in size can be achieved.

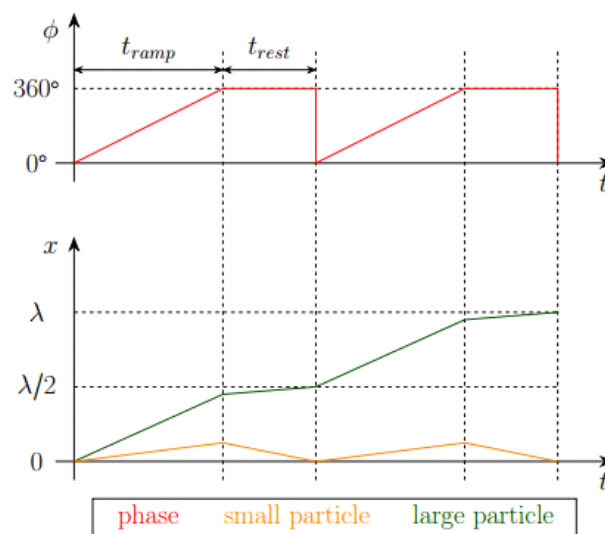


Figure. 1. Principle of dynamic acoustic standing wave sorting technique. Top graph shows phase shift;  $t_{ramp}$  is the time duration over which the phase is changed,  $t_{rest}$  is the time duration for the constant phase. The bottom graph shows the resulting lateral displacement over time that particles experience depending on their size. The large particles will follow the shifted acoustic field while the small particles will stay at their initial position. The wavelength of the signal is  $\lambda$ .

### 2.3. Acoustic tweezers and experimental setup

The acoustic tweezer used was a surface acoustic wave device with a polydimethylsiloxane (PDMS) micro-channel. The interdigitated transducers (IDTs) were fabricated on a 1 mm thick  $128^\circ$  Y-cut lithium niobate wafer using chromium/gold deposition and lift-off. The width of the electrode fingers and spacing were chosen to be  $75 \mu\text{m}$ , resulting in a wavelength of  $300 \mu\text{m}$  and theoretical operating frequency of 12.6 MHz. The polydimethylsiloxane (PDMS) channel was fabricated via soft lithography. The main channel is  $50 \mu\text{m}$  in height,  $240 \mu\text{m}$  in width and has a length of 2 cm. The inlets have an asymmetric arrangement to facilitate focusing and alignment of particles prior to sorting: two inlets are  $50 \mu\text{m}$  in width and one on the side is  $140 \mu\text{m}$  as shown in Fig. 2. The two parts of the device were bonded after a mixed oxygen plasma treatment, using a corona gun and reactive ion etching [26]. The surface of the PDMS channel was activated for 30 s at medium power using the discharge gun. A small amount of methanol was applied on the substrate prior to bonding to allow for positioning of the PDMS [27]. The activated surfaces bond to each other after the methanol evaporates.

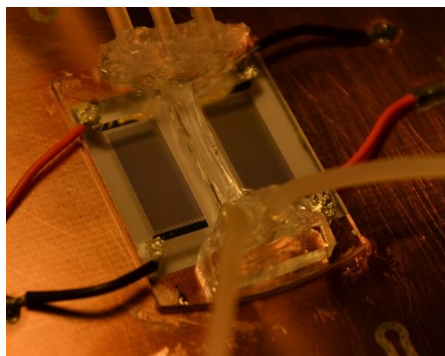


Figure 2. Photograph of surface acoustic wave device with a bonded PDMS microfluidic channel on a printed circuit board.

The experimental setup comprised the device mounted on a printed circuit board (PCB), three syringes to provide sheath flow and the flow of the particles, syringe pumps (World Precision Instruments, Sarasota, USA), a signal generator (TG5012A, Aim-TTi, UK) and power amplifiers (ZHL-1-2W+, Mini-Circuits, UK). The appropriate phase pattern and signal parameters were uploaded to the signal generator via a general-purpose interface bus connection using LabView (National Instruments). The flow rates of the syringes were varied until a dense single line of particles could be observed at one side of the centerline of the channel. The distance between the centerline and the particle flow was adjusted to be a quarter of the wavelength ( $71\ \mu\text{m}$ ), therefore after successful separation the two types of particles would be located symmetrically on the two sides. To achieve these requirements the sheath flow in the  $50\ \mu\text{m}$  wide channel was adjusted to  $0.45\ \mu\text{l}/\text{min}$ , the particle flow  $0.2\ \mu\text{l}/\text{min}$ , and the sheath flow in the  $140\ \mu\text{m}$  wide inlet channel was  $2.5\ \mu\text{l}/\text{min}$ .

### 3. Results and discussions

#### 3.1 Particle separation by switchable custom made polymer microspheres

The polymer microspheres were synthesized in a single preparative step by the precipitation polymerisation of a dilute solution of divinylbenzene-55 (DVB-55) in a mixture of acetonitrile and toluene ( $7/3\ [\text{v}/\text{v}]$ ), with the radicals required for the free radical polymerisation being generated through the thermal decomposition of azobisisobutyronitrile (AIBN). Precipitation polymerization [28] is a very convenient synthetic method for the production of high quality polymer microspheres with mean diameters normally in the range  $0.1 - 10$  micrometres. Typically, the method involves the polymerisation of vinyl monomers in dilute solution (monomer concentration typically  $< 5\% \text{ w}/\text{v}$ ) in a near-theta solvent. The particle size can be controlled with ease (since the mechanism of precipitation polymerisation is one of nucleation and growth), the polymerisation conditions can be tuned to impart porosity into the microspheres if so desired, and functional groups can be installed into the particles via either copolymerisation or post-polymerisation chemical modification strategies. Furthermore, unlike emulsion and suspension polymerisation, precipitation polymerisation does not require the use of surfactants/stabilisers so the microspheres produced are clean and free of surface contaminants.

When changing the contrast factor by alternating the ethanol concentration of the aqueous solution, the custom made fabricated micro-particles were able to be shifted from the node to antinode, while the commercialised polystyrene micro-particles (Polysciences, UK) stayed at the acoustic node position. Figure 3(a) illustrates  $10\ \mu\text{m}$  commercialised and  $4.6\ \mu\text{m}$  custom made micro-particles at the node position when the concentration of ethanol was at  $70\%$ , exhibiting a positive contrast factor. Figure 3(b) illustrates the  $10\ \mu\text{m}$  commercialised and  $4.6\ \mu\text{m}$  custom made micro-

particles at node and antinode positions respectively, when the concentration of ethanol was of 35%, and the custom made micro-particles exhibited a negative contrast factor.

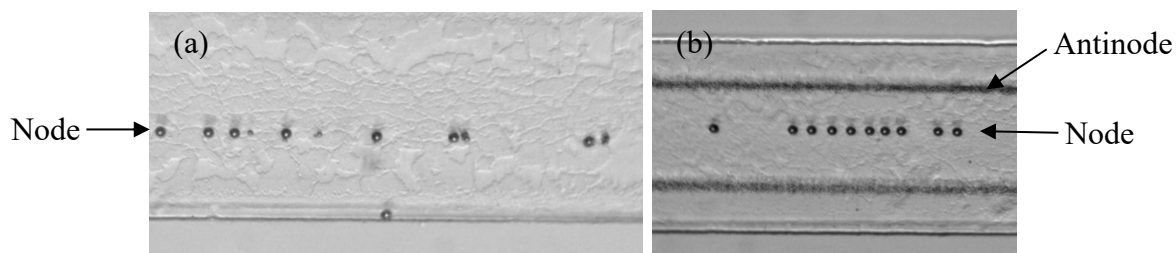


Figure 3. 10  $\mu\text{m}$  commercialised and 4.6  $\mu\text{m}$  custom made micro-particles aligned (a) at the nodal position of the surface acoustic standing wave, (b) at the node and antinode positions of the surface acoustic standing wave, respectively.

### 3.2 Particle separation by dynamic acoustic standing waves

Experiments for separation of 15 and 10  $\mu\text{m}$  commercialised polystyrene particles (Polysciences, UK) have been carried out (Fig. 4) and particle traces were recorded. The applied voltage on the IDTs was 23 V. For this excitation, we observed separation for ramping times between 0.6 and 1 s, having the best efficiency of separation when 0.7 s was used. For this ramping time, 100 % of the target particles reached the bottom outlet, while 94.5 % of the small particles stayed in the waste collection outlet.

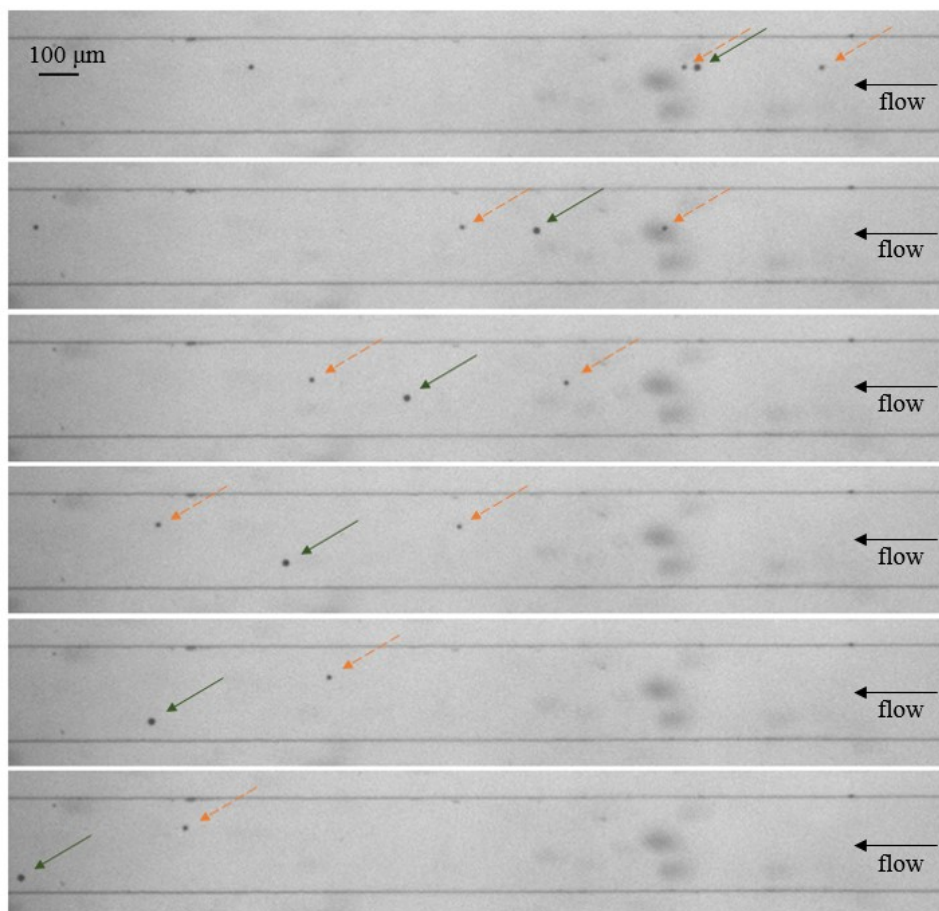


Figure 4. Images showing the separation process for 0.7 s ramping time. The 15 (green, solid) and 10 (orange, broken)  $\mu\text{m}$  particles enter from the top right and the larger one is shifted to the bottom. The flow is from the right to the left. The frames are taken every 0.3 s.



Figure 5 shows the transversal displacement of 15 and 10  $\mu\text{m}$  polystyrene particles over time. It can be seen that the large particle follow the shifted acoustic field during  $t_{\text{ramp}}$ , while the smaller particles stay at their initial position. During  $t_{\text{rest}}$ , the large particles relax at the next node while the smaller one relax at the initial node position.

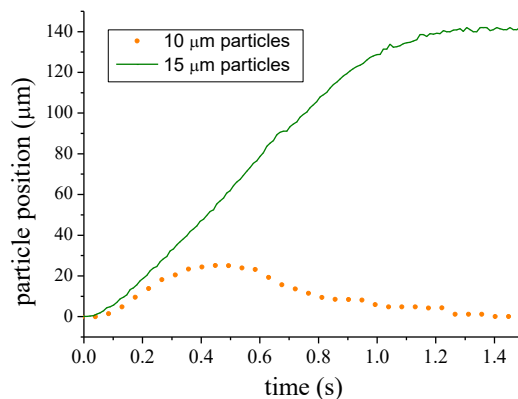


Fig. 5. Experimental results for separating 15 and 10  $\mu\text{m}$  polystyrene particles.

## 4. Conclusion

In this paper, we demonstrated the application of surface acoustic standing wave for separating particles. The first method relies on changing the acoustic contrast factor and the custom made micro-particle move from node to antinode of the acoustic pressure. The second method relies on shifting the phase of the acoustic standing wave and taking advantage of the different scaling forces applied to the micro-particles. The large micro-particles follow the shifted acoustic field while the smaller particles stay at their initial position. Both methods showed very good separation performance, up to 100%. The custom made switchable particles could be used as drug carriers for targeted drug delivery applications. Dynamic acoustic standing waves can be used for acoustic cytometry in sorting fragile biological living cells.

## 5. Acknowledgement

The authors would like to thank Neil Ross and Dr William N MacPherson for advising us on clean room equipment and giving us access to material deposition.

## REFERENCES

1. Yu, L., et al., *Advances of lab-on-a-chip in isolation, detection and post-processing of circulating tumour cells*. Lab Chip, 2013. **13**(16): p. 3163-82.
2. Augustsson, P., et al., *Microfluidic, label-free enrichment of prostate cancer cells in blood based on acoustophoresis*. Anal Chem, 2012. **84**(18): p. 7954-62.
3. Bernassau, A.L., et al., *Direct patterning of mammalian cells in an ultrasonic heptagon stencil*. Biomed Microdevices, 2012. **14**(3): p. 559-64.
4. Yahya, W.N., N.A. Kadri, and F. Ibrahim, *Cell patterning for liver tissue engineering via dielectrophoretic mechanisms*. Sensors (Basel), 2014. **14**(7): p. 11714-34.
5. Pommer, M.S., et al., *Dielectrophoretic separation of platelets from diluted whole blood in microfluidic channels*. Electrophoresis, 2008. **29**(6): p. 1213-8.
6. Cheng, I.F., et al., *A continuous high-throughput bioparticle sorter based on 3D traveling-wave dielectrophoresis*. Lab on a Chip, 2009. **9**(22): p. 3193-3201.

7. Adams, J.D., U. Kim, and H.T. Soh, *Multitarget magnetic activated cell sorter*. Proc Natl Acad Sci U S A, 2008. **105**(47): p. 18165-70.
8. Bragheri, F., et al., *Optofluidic integrated cell sorter fabricated by femtosecond lasers*. Lab Chip, 2012. **12**(19): p. 3779-84.
9. Wang, X., et al., *Enhanced cell sorting and manipulation with combined optical tweezer and microfluidic chip technologies*. Lab Chip, 2011. **11**(21): p. 3656-62.
10. Wiklund, M., *Acoustofluidics 12: Biocompatibility and cell viability in microfluidic acoustic resonators*. Lab Chip, 2012. **12**(11): p. 2018-28.
11. Bernassau, A.L., et al., *Interactive manipulation of microparticles in an octagonal sonotweezer*. Applied Physics Letters, 2013. **102**(16): p. 164101.
12. Devendran, C., I. Gralinski, and A. Neild, *Separation of particles using acoustic streaming and radiation forces in an open microfluidic channel*. Microfluidics and Nanofluidics, 2014. **17**(5): p. 879-890.
13. Franke, T., et al., *Surface acoustic wave actuated cell sorting (SAWACS)*. Lab Chip, 2010. **10**(6): p. 789-94.
14. Ding, X., et al., *Cell separation using tilted-angle standing surface acoustic waves*. PNAS, 2014. **111**(36): p. 12992–12997.
15. Jo, M.C. and R. Guldiken, *Active density-based separation using standing surface acoustic waves*. Sensors and Actuators A: Physical, 2012. **187**: p. 22-28.
16. Skowronek, V., R.W. Rambach, and T. Franke, *Surface acoustic wave controlled integrated band-pass filter*. Microfluidics and Nanofluidics, 2015. **19**(2): p. 335-341.
17. Ding, X., et al., *On-chip manipulation of single microparticles, cells, and organisms using surface acoustic waves*. Proc Natl Acad Sci U S A, 2012. **109**(28): p. 11105-9.
18. Drinkwater, B.W., *Dynamic-field devices for the ultrasonic manipulation of microparticles*. Lab Chip, 2016. **16**(13): p. 2360-75.
19. Franke, T., et al., *Numerical simulation of surface acoustic wave actuated cell sorting*. Open Mathematics, 2013. **11**(4).
20. Llewellyn-Jones, T.M., B.W. Drinkwater, and R.S. Trask, *3D printed components with ultrasonically arranged microscale structure*. Smart Materials and Structures, 2016. **25**(2): p. 02LT01.
21. Glynne-Jones, P., et al., *Mode-switching: a new technique for electronically varying the agglomeration position in an acoustic particle manipulator*. Ultrasonics, 2010. **50**(1): p. 68-75.
22. Harris, N., et al., *A novel binary particle fractionation technique*. Physics Procedia, 2010. **3**(1): p. 277-281.
23. Ding, X., et al., *Standing surface acoustic wave (SSAW) based multichannel cell sorting*. Lab Chip, 2012. **12**(21): p. 4228-31.
24. Yosioka, K. and Y. Kawasima, *Acoustic radiation pressure on a compressible sphere*. Acta Acustica united with Acustica, 1955. **5**(3): p. 167-173.
25. Petersson, F., et al., *Separation of lipids from blood utilizing ultrasonic standing waves in microfluidic channels*. Analyst, 2004. **129**(10): p. 938-43.
26. Johansson, L., et al., *Surface acoustic wave induced particle manipulation in a PDMS channel--principle concepts for continuous flow applications*. Biomed Microdevices, 2012. **14**(2): p. 279-89.
27. Shi, J., et al., *Continuous particle separation in a microfluidic channel via standing surface acoustic waves (SSAW)*. Lab Chip, 2009. **9**(23): p. 3354-9.
28. Li, K. and Stover, H.D.H., *Synthesis of Monodisperse Poly (divinylbenzene) Microspheres*. Journal of Polymer Science: Part A Polymer Chemistry, **31**(13): 3257-63.